



Published in final edited form as:

Exp Eye Res. 2022 January ; 214: 108891. doi:10.1016/j.exer.2021.108891.

An ex vivo model of human corneal rim perfusion organ culture

Michael Peng^a, Tyler J. Margetts^a, Chenna Kesavulu Sugali^a, Naga Pradeep Rayana^a,
Jiannong Dai^a, Tasneem P. Sharma^{a,b}, Vijay Krishna Raghunathan^{c,d}, Weiming Mao^{a,b,e}

^aEugene & Marilyn Glick Eye Institute, Department of Ophthalmology, Indiana University School of Medicine

^bDepartment of Pharmacology and Toxicology, Indiana University School of Medicine

^cThe Ocular Surface Institute, Department of Basic Sciences, College of Optometry, University of Houston

^dDepartment of Biomedical Engineering, Cullen College of Engineering, University of Houston

^eDepartment of Biochemistry and Molecular Biology, Indiana University School of Medicine

Abstract

The human anterior segment perfusion culture model is a valuable tool for studying the trabecular meshwork (TM) and aqueous humor outflow in glaucoma. The traditional model relies on whole eye globes resulting in high cost and limited availability. Here, we developed a glue-based method which enabled us to use human corneal rims for perfusion culture experiments. Human corneal rim perfusion culture plates were 3D printed. Human corneal rims containing intact TM were attached and sealed to the plate using low viscosity and high viscosity glues, respectively. The human corneal rims were perfused using the constant flow mode, and the pressure changes were recorded using a computerized system. Outflow facility, TM stiffness, and TM morphology were evaluated. When perfused at rates from 1.2 to 3.6 $\mu\text{l}/\text{min}$, the outflow facility was 0.359 ± 0.216 $\mu\text{l}/\text{min}/\text{mmHg}$ among 10 human corneal rims. The stiffness of the TM in naïve human corneal rim was similar to that of perfusion cultured human corneal rim. Also, the stiffness of TM of corneal rims perfused with dexamethasone was significantly higher than the control. Human corneal rims with glue contamination in the TM could be differentiated by high baseline intraocular pressure as well as high TM stiffness. Histology studies showed that the TM tissues perfused with plain medium appeared normal. We believed that our glued-based method is a useful tool and low-cost alternative to the traditional anterior segment perfusion culture model.

Correspondence author: Weiming Mao Ph.D., Associate Professor, Eugene and Marilyn Glick Eye Institute, Department of Ophthalmology, Department of Pharmacology and Toxicology, Department of Biochemistry & Molecular Biology, Indiana University School of Medicine, RM305V, 1160 W. Michigan St, Indianapolis, IN, 46202, USA, weimmao@iu.edu, [1-317-278-0801](tel:1-317-278-0801).

Publisher's Disclaimer: This is a PDF file of an unedited manuscript that has been accepted for publication. As a service to our customers we are providing this early version of the manuscript. The manuscript will undergo copyediting, typesetting, and review of the resulting proof before it is published in its final form. Please note that during the production process errors may be discovered which could affect the content, and all legal disclaimers that apply to the journal pertain.

Keywords

Anterior segment perfusion culture; Aqueous humor outflow; Corneal rim; Stiffness; Trabecular meshwork

1. Introduction

Primary open angle glaucoma (POAG) is the most common form of glaucoma, a leading cause of blindness worldwide (Resnikoff et al., 2004). In POAG, elevated intraocular pressure (IOP) is the primary modifiable risk factor (AGIS, 2000). IOP is maintained by a homeostatic balance between aqueous humor secretion by the ciliary body and its drainage through the aqueous humor outflow pathway. Most of the aqueous humor drainage occurs at the conventional pathway through the trabecular meshwork (TM) pathway, and a minority occurs through the unconventional uveoscleral pathway (Ellingsen and Grant, 1971; Stamer and Acott, 2012). Impaired outflow facility through the TM disrupts aqueous humor drainage and leads to increased IOP (Stamer and Acott, 2012). The TM tissue consists of TM cells in a three-dimensional extracellular matrix (ECM) including beams and loose connective tissue (Keller et al., 2018; Stamer and Clark, 2017). Glaucomatous TM changes include loss of TM cells, impaired TM functions, excessive deposition of extracellular matrix, and elevated TM stiffness, which contribute to increased aqueous humor outflow resistance. Although these pathologic changes are well recognized, the exact mechanism of POAG TM pathology is not entirely clear.

To study physiology and pathology of the TM, many research models have been developed including *in vitro* models (TM cell cultures (2D) (Keller et al., 2018), 3D cell culture (Li et al., 2020), cell derived matrices (Yemanyi et al., 2020), flow mimicking devices (Torrejon et al., 2013)) and *in vivo* models (mice, rats, rabbits, sheep, cows, and primates) (Shepard et al., 2010) (Gerometta et al., 2004; Gerometta et al., 2009; Lorenzetti, 1970; Rasmussen and Kaufman, 2005; Shepard et al., 2010). Besides these two groups of models, the *ex vivo* models are another important research model. *Ex vivo* models include non-perfusion and perfusion anterior segment cultures. In non-perfusion cultures, the anterior segment/corneoscleral rim was either cultured as a whole piece (Acott et al., 1988) or as quadrants after dissection (Kasetti et al., 2020) in static culture medium. This method is easy to set up and have been used for morphological and biochemical analysis (Acott et al., 1988; Kasetti et al., 2020). However, non-perfusion cultures do not provide physiology data including IOP. In contrast, in perfusion cultures, the entire anterior segment is sealed onto a device and culture medium is constantly perfused into the anterior chamber. Perfusion cultures mimic physiological aqueous humor outflow and provide outflow data. Due to these advantages, anterior segment perfusion cultures, especially the human anterior segment perfusion organ culture models have been widely used (Johnson and Tschumper, 1987). The anterior segment perfusion culture model has been valuable in understanding aqueous humor dynamics, conducting outflow facility experiments, in isolating and understanding segmental flow, in modeling pathologic parameters, as well as in developing a better understanding of the morphologic, ultrastructural, molecular, biomechanical, and biochemical changes in the TM using native biological tissue.

Dr. Douglas Johnson and colleagues first established the human anterior segment perfusion culture model (Johnson and Tschumper, 1987). The current models are all based on his original design with some modifications. In this type of models, the human donor eye is bisected at the equator. After removal of the uveal tract, retina, lens, the dome shaped tissue containing only the cornea, sclera and TM is mounted on a custom-made dish. A rigid ring is used to clamp the tissue against the dish at the sclera, and the ring is secured using screws. Since the sclera is compressible, it functions as an intrinsic washer/gasket which, together with the dish and ring, forms a watertight artificial anterior chamber. The sclera close to the limbus is usually gently scored, which cuts off the episcleral veins allowing perfusion medium (mimicking the aqueous humor) to drain. The dish has two pre-drilled tunnels, one for medium infusion and the other for pressure recording. Experimental treatments such as growth factors, compounds, vectors can be delivered onto the ocular surface (eyedrops) or infused through the tunnel. This model can be run at constant perfusion mode or constant pressure mode. Under constant perfusion mode, the anterior segment is perfused at a constant flow rate (different rates can be applied per experimental design) using a syringe pump and IOP is monitored using a pressure transducer (Mao et al., 2011). Under constant pressure mode, there are a few approaches: 1) The anterior segment is perfused using a raised medium reservoir (hydrostatic pressure; adjustable by varying heights) and flow rate is monitored by weighing the perfusion set (the change in weight due to displacement of medium represents the amount of medium outflow) (Abu-Hassan et al., 2015). 2) To set up a feedback control system in which the pressure transducer provides feedback signal to the computer which further determines and regulates the syringe pump to provide required flow rate (Comes and Borrás, 2009). This flow rate is also constantly monitored and recorded by the computer. 3) Similar to the 1st method, IOP is maintained using a medium reservoir but flow rate is monitored using a flow sensor (Sherwood et al., 2016).

Human, porcine, and bovine eyes have been used for perfusion culture studies (Johnson and Tschumper, 1987; Loewen et al., 2016; Mao et al., 2011). Among these models, the human donor eye model is the most relevant since the anatomy and physiology of the TM of porcine and bovine eyes are different from those of human eyes. For example, porcine and bovine eyes do not have authentic Schlemm's canal, and they show washout effects (Johnson et al., 1991; Overby et al., 2002; Zhou et al., 2017), i.e. a transient decrease in resistance to outflow with increasing volume of perfusate, unlike human eyes (Erickson-Lamy et al., 1991; Erickson-Lamy et al., 1990).

However, the use of human anterior segments for perfusion culture in glaucoma research is limited because whole donor eye globes are needed. Procuring whole globes is challenging and expensive. Also, they are not always readily available since most of the donor eyes are prioritized for transplantation or corneal rim collection. In contrast, the human corneal rim tissue is more affordable with a relatively greater supply from eye banks. Thus, using human corneal rims for perfusion experiments would greatly increase the access and usage of donor tissues in a cost-effective manner. Here, we developed a modified perfusion chamber with reduced footprint to accommodate corneal rims, and the corneal rims were mounted using a glue-based approach. This model/method enabled us to reduce/replace our dependency on human whole globes for TM research.

2. Materials and supplies

Human donor corneal rims (Saving Sight, Kansas City, MO)

CO2 incubator

PBS buffer

Opti-MEM (Thermo Fisher Scientific)

Surgical scalpels, forceps, scissors (Any generic brands)

Q-tips

Gauze pads

Perfusion plates: 3D printed using Formlab 3 printer and Formlab transparent resin (catalog#: RS-F2-GPCL-04) (Somerville, MA)

Plate Holders: the 3D printed part was glued to a segment of 1.5 inch PVC pipe with side cut Stainless Steel 316 Hypodermic Tubing, 20 Gauge (Amazon; Seattle, WA): the tubing was cut to about 2cm and glued to the two holes in the perfusion plate using Epoxy at least 1 day before.

Plastic tubing (Catalog#: AAD04119; Tygon, Malvern, PA)

20 gauge Hypodermal needles (blunt end) (Catalog#:427564; BD, Sparks, MD)

20ml plastic syringes (Any generic brands)

Perfusion pump (F200X; Chemyx, Stafford, TX)

Pressure transducers (Catalog#: MLT0670; AdInstruments, Colorado Springs, CO)

2-way stopcocks (Catalog#: 99745; Qosina, Ronkonkoma, NY)

Stopcock plugs (Catalog#: 65818; Qosina)

Glutire tissue glue (Catalog#: NC9855218; Fisher scientific, Waltham, MA)

Loctite Super Glue ([Amazon.com](https://www.amazon.com), Seattle, WA)

Contact lens (Expired contact lens from a variety of manufacturers)

100mm petri dishes (Fisher scientific)

Punch (Catalog#: 66010; McMaster-Carr; Elmhurst, IL)

PowerLab bridge amplifier (Catalog#: FE228) and amplifier (PL3508/P) (AdInstruments)

Adapter cables (Catalog#: MLAC06; AdInstruments)

LabChart software (included with hardware; AdInstruments)

Laptop computer

3D printing files: see Supplemental Data 1 and 2

3. Detailed methods

A video showing the entire procedure was included (Supplemental video 1 and Supplemental Figure 1).

3.1. Corneal rim perfusion culture setup

Human donor corneal rims were obtained from the eye bank (Saving Sight, Kansas City, MO) and processed within 3-7 days postmortem. Paired and unpaired corneal rims were used. The corneal rims were from Caucasian and African American donors. Corneal rims less than 18mm in diameter, with significant corneal defects, or positive serologies for hepatitis, HIV, or COVID-19 were excluded.

The main challenge in using corneal rim tissues for perfusion culture is that there is not sufficient amount of sclera for clamping using the Johnson's method. We tried to modify the size of the central elevation of the dish to fit the sclera. However, the baseline IOP was very high (could reach >50mmHg), indicating that the TM was physically clamped (data not shown). Therefore, we designed a perfusion plate with grooves. The corneal rim was glued onto the plate to form a watertight anterior chamber for perfusion culture.

The overall setup for our perfusion culture model is shown in Figure 1. The residual uveal tract tissues were removed from the corneal rim by gentle scraping using a surgical blade. An 18mm punch (MayhewPro, Turners Falls, MA) was then used to mark the sclera for the perfusion plate and excess scleral tissue was trimmed. The corneal rim was rinsed briefly with PBS and subsequently placed on a dry gauze pad. Both the inner and outer sides of the sclera were dried by wiping the tissue with sterile Q-tips. During this procedure, the TM region was not wiped to avoid damage. The inner and outer sides of the scleral approximately 1.5mm posterior to the TM/limbus were gently scored using a surgical blade or a diamond knife. This procedure created an additional barrier to prevent glue from potentially spreading anteriorly and obstructing the TM or limbal regions. Also, scoring the limbal region (outside) allowed the medium to drain because the episcleral veins were cut. With the perfusion dish seated within the holder, the GLUture tissue adhesive (Zoetis Inc., Kalamazoo, MI) was distributed evenly within the depression/groove on the perfusion plate. The prepared corneal rim was then mounted onto the perfusion dish, ensuring that the exposed scleral edge was evenly seated within the adhesive-filled depression/groove. Forceps were used to apply light pressure on the outer side of the sclera to ensure proper seal. Once fully adjusted, a sterile soft contact lens was dried of excess solution and placed over the cornea, ensuring the entire limbal region was evenly protected. Gel Super Glue (Loctite Ultra Gel Control, Amazon, WA, USA) was then evenly applied around the circumference of the scleral edge to create a complete seal. The glue was allowed to polymerize in the cell culture incubator for 2 hours. The moisture in the incubator prevented

cornea from drying and accelerated glue polymerization. After 2 hours, perfusion was set up by connecting plastic tubing to stainless steel tubing on the plate to two syringes. The air in the anterior chamber and tubing was carefully removed by doing a “push and pull” using two syringes with one “push” syringe filled with Opti-MEM supplemented with 1% glutamine and 1% penicillin/streptomycin (Thermo Fisher Scientific), and the other empty “pull” syringe being used to remove air. After connecting the tubing with the pressure transducer (MLT0670; AdInstruments, Colorado Springs, CO) and the programmable syringe pump (F200X; Chemyx, Stafford, TX) medium was infused using the syringe pump at different perfusion rates and IOP was recorded using the pressure transducer, PowerLab amplifier, Octal Bridge Amplifier as well as the LabChart software (AdInstruments). IOP was sampled once per 1 or 30 seconds.

During this procedure, we found that glue might be drawn into the TM region likely due to the capillary effect. To prevent glue contamination, we gently scored the sclera distal to the TM region to create a tissue flap. Also, in the initial experiment, we observed that during gel glue polymerization, polymerized glue formed on top of the cornea, which was probably due to evaporation. Therefore, in subsequent experiments, we routinely placed a contact lens on the cornea (right before application of Gel Super Glue) to prevent glue contamination during polymerization and equilibration. Also, after setup and initiation of perfusion, we recommend allowing any residual uncured glue and vapor to cure or dissipate overnight.

Here is a summary of setup flow (also see Supplemental video 1 and Supplemental Figure 1): Prepare the cornea → glue the cornea to the plate using GLUture → cover with contact lens → Gel Super glue to seal the cornea → 2 hour polymerization (no perfusion) in the incubator → setup perfusion and pressure transducer → perfusion overnight → remove contact lens → perfusion for one more day to establish baseline IOP before outflow facility measurement/treatment.

3.2. Outflow facility and IOP measurement

To obtain outflow facility, we perfused the corneal rims at different flow rates in a stepwise manner with 75 minutes per step, and IOP was recorded (Figure 2). We observed that IOP equilibration could often be achieved within 30 minutes. Ten of twelve corneal rims were used for outflow facility measurements (Figure 3A). The excluded corneal rims demonstrated persistently high baseline pressures (usually >40mmHg) likely due to glue contamination.

The perfusion culture system was first equilibrated at a physiologic flow rate of 2.4 $\mu\text{l}/\text{min}$ for at least 24 hrs. Perfusion was conducted in a sterile, humidified chamber maintained at 37°C. The contact lens was removed prior to the experiment. An automated stepwise program was initiated using the syringe pump. Starting at 1.2 $\mu\text{l}/\text{min}$, the flow rate was increased to 3.6 $\mu\text{l}/\text{min}$ at an interval of 0.4 $\mu\text{l}/\text{min}$ at 75 min per interval. A rolling average of the last 15 minutes prior to a flow rate change was used for data analysis.

Outflow facility was calculated using the Goldmann equation ($\text{IOP} = \text{F}/\text{C} + \text{P}_e$, F = inflow rate or aqueous humor production rate, C = outflow facility, P_e = episcleral venous pressure). In our model, the episcleral venous pressure was set at zero. We found that with an increase

in flow rates, the measured facility increased, and this was validated with a linear regression ($N=9$ or 10 ; $r^2=0.92$) (Figure 3B). Overall, we obtained an outflow facility of 0.359 ± 0.216 $\mu\text{l}/\text{min}/\text{mmHg}$ (mean \pm standard deviation; $N=10$) (Figure 3C).

3.3. TM morphology after perfusion culture

In order to assess the integrity of the TM structures after perfusion, three representative corneal rims were used for histologic analysis (Figure 4). The corneal rims were cut into four 3mm sagittal sections and individually fixed in 4% paraformaldehyde in PBS at 4°C overnight. The tissues were rinsed with PBS, dehydrated, and embedded in paraffin. Tissue samples were sectioned at $5\mu\text{m}$ in thickness and processed for staining with hematoxylin and eosin. Images were captured using the Nikon Ti2 microscope (Nikon Instruments Inc, Melville, NY).

Due to the close proximity of the TM region and the scleral edge in the corneal rim model, proper application of glue and proper mounting of the corneal rim on the perfusion plate were important to prevent glue contamination of the TM region. The active ingredient in the adhesives, cyanoacrylate, polymerizes rapidly in the presence of moisture. Initial experiments showed that these glues spread anteriorly toward the cornea and obstruct the TM and limbus. Circumferential partial thickness incisions on both the inner and outer sclera provided a barrier and helped to decrease glue contamination of the TM region (Figure 1E). A soft contact lens placed on the cornea provided an additional protection of the limbus while keeping the cornea moist. With the help of these two techniques, we increased the chance of obtaining glue-free, well preserved TM structures after perfusion.

3.4. The perfusion model is suitable for studying TM stiffness

After perfusion, the corneal rims were removed from the perfusion plate using a surgical blade at IUSM and shipped overnight in Optisol (Chiron Intraoptics, Irvine, CA, USA) to UHCO for mechanical characterization. Some corneal rims were not removed and the entire sets were shipped directly to UHCO, and the tissues were removed at UHCO. The TM was dissected from the corneal rims and mounted with the juxtacanalicular region (JCT) side up in an AFM dish coated with a thin layer of Sylgard 527 as described elsewhere (Morgan et al., 2014). Force-distance curves were obtained from 5-10 locations per tissue sample with 3 force curves per location using a Bruker BioScope Resolve AFM in contact mode, in fluid, using a silicon-nitride cantilever modified with a borosilicate bead with nominal diameter ($1-2\mu\text{m}$) and calibrated for spring constant and deflection sensitivity using a glass slide. Elastic moduli were determined for a spherical indenter as described previously (Chang et al., 2014; McKee et al., 2011).

First, we compared the modulus of naïve TM tissues (not perfused) to the TM tissue from the fellow corneal rim which was perfused and showed an IOP $>60\text{mmHg}$. Under light microscopy, we found that some TM tissues in perfused corneal eyes had minor or severe glue contamination (Figure 5A). Atomic force microscopy showed that glue contamination (Glue A: 893 ± 98.98 kPa; Glue-B: 4.116 ± 1.723 kPa; mean \pm standard deviation) significantly increased TM stiffness in comparison with naïve tissue (1.201 ± 0.78 kPa; mean \pm standard deviation), suggesting the prevention of glue contamination is important for

establishing this model even though there may be regions where glue permeation is minimal within the same sample.

Second, we compared elastic modulus of the TM from paired corneal rims with or without perfusion (Figure 5B). The perfusion cultured corneal rim did not show high IOP (about 2-3mmHg throughout perfusion). We found that perfusion culture of the corneal rim did not change TM stiffness (Naïve: 2.55 ± 1.05 kPa; Perfused: 1.92 ± 0.64 kPa; mean \pm standard deviation), which validates our model.

Last, we perfusion cultured two pairs of corneal rims, one with 0.1% ethanol (vehicle) and the fellow rim with 100nM dexamethasone. We found that dexamethasone treated eyes showed significantly higher stiffness (hTM2973: 2.39 ± 1.34 kPa vs 6.07 ± 2.2 kPa; hTM3009: 1.98 ± 0.82 kPa vs 8.39 ± 4.27 kPa; mean \pm standard deviation) in the TM (Figure 5C).

4. Potential pitfalls and trouble shooting

We established a new perfusion culture model using the human corneal rim tissue. This model is easy to set up and we were successful in 10 of 12 (i.e. 83% of samples) corneal rims. Specifically, we demonstrate the feasibility of the model in the study of outflow facility, monitoring IOP changes, and maintaining an intact histology of the TM. The measured outflow facility was within published ranges for human eyes (Acott et al., 2014b; Cha et al., 2016; Erickson-Lamy et al., 1991; Erickson-Lamy et al., 1990; Kazemi et al., 2018; McDonnell et al., 2018; Raghunathan et al., 2018), and this model is sensitive enough for studying TM stiffness changes. Although the increase in TM stiffness after dexamethasone treatment was still within the normal range of low flow regions, (Raghunathan et al., 2018; Vranka et al., 2018) the purpose of this study was not to evaluate the effects of drugs, but to demonstrate the feasibility of the perfusion system. Since a small sample size was utilized to determine feasibility, and no labeling of segmental flow regions was performed, any relationship inferred between dexamethasone and tissue stiffness needs to be done so with abundant caution. Due to the advantages of this model (listed below), future studies will focus on studying various aspects of TM outflow and physiology including but not limited to biomechanics, changes in protein expression, segmental flow, effects of drugs, and/or effects of gene overexpression/knockdown.

4.1 The advantages of this model include:

a. Minimal mechanical stress on tissues.—In the Johnson's model, a clamping O-ring is mounted on top of the sclera to compress the eye in order to create a watertight seal. However, it is difficult to accommodate such a device on the limited scleral tissue for the corneal rim without depressing the natural convexity of the cornea and inducing additional strain on the TM region. Gluing the scleral edge induces minimal mechanical stress on the relevant tissues.

b. Cost and availability—In comparison to whole eyes, corneal rims are generally more affordable and available at the eye bank. Also, it is generally believed that whole eyes need to be processed within 2 days post-mortem for optimal results. This short time window

is because whole eyes are usually wrapped in humid gauze pads. Even when whole eyes are preserved in culture medium, the intact sclera forms a barrier which limits the access of medium to intraocular tissues, including the TM. In contrast, the corneal rim has been dissected so that the TM as well as corneal endothelia are directly immersed in corneal preservation medium like Optisol. Corneal rims, when preserved in Optisol, are good for corneal transplantation up to 2 weeks (Lindstrom et al., 1992). Our experience is that corneal rims up to at least 7 days in preservation medium can still generate good results.

c. Simplicity of experimental setup—Processing time for the corneal rim was significantly shorter than the whole eye as a result of fewer tissues to dissect. A crucial step for any perfusion organ culture model is to ensure a tight seal between the tissue and the perfusion device. In the anterior segment model, close attention must be made to the seating of the O-ring such that even pressure is applied to the sclera. In contrast, a proper seal could be obtained with the corneal perfusion model by ensuring complete coverage by the glue.

d. Easy production—Since we used perfusion plates, they require very little 3D printing materials and greatly shortens printing time. With the modern 3D printing devices, large scale production of these devices in house has become possible.

e. Space saving—Since we utilize perfusion plates *in lieu* of large perfusion chambers in conjunction with a greater number of rims, we can theoretically increase the number of perfusion systems within a limited space in an incubator. We would only be limited by our ability to multiplex the number of syringe pumps / pressure transducers.

4.2 The disadvantages of this model include:

a. Inability to adjust the corneal rim after mounting—After the glue has fully set, the corneal tissue can no longer be adjusted if there is any suspected obstruction or improper positioning of the organ culture. The perfusion plates can only be used once per eye as a consequence of the gluing protocol.

b. Risk of obstruction—Obstruction of the TM region could occur primarily in several ways. During the mounting of the corneal rim, there is a risk of unintentional contact with the tissue glue which will immediately begin to polymerize due to the residual moisture retained by the cornea. Obstruction can also occur after mounting. If the glue is not properly set before perfusing the eye with medium, the glue could be released into the artificial anterior chamber and partially obstruct TM regions. Additionally, migration of the glue anteriorly towards the TM and limbus region could occur after mounting. Properly drying the inner and outer sclera as well as creating the circumferential partial thickness scleral flap is critical to prevent this adverse effect. We identified two of the twelve eyes with likely glue contamination based on their high baseline IOP (>40mmHg). These were excluded from outflow facility measurements.

c. Additional time for glue polymerization—Before the eye can be perfused with medium, the glue must be allowed to set. In our protocol, we found that 2 hours incubation

in a culture incubator was sufficient. In contrast, the anterior segment bisected from the whole globe can be perfused immediately after clamping.

d. Large variations in outflow facility—Our data showed that perfusion cultured corneal rims showed consistent outflow facilities within the range of 1.2 to 3.2 $\mu\text{l}/\text{min}$ perfusion rate. However, if outflow facility was calculated based on individual eyes and pooled, we found that the outflow facility range was relative wide. However, in the anterior segment perfusion culture system, it is not uncommon (Snider et al., 2021). This relatively wide range could be due to the freshness of the tissue, age of the donor, unknown ocular medical history, and differences in the procedure. However, as long as a stable baseline IOP is established and the IOP changed is compared to the baseline, this difference in baseline IOP/physiological outflow facility is no longer important due to the self-control (baseline IOP). Further, we noted that outflow facility measurements closely followed increases in perfusion rate. This suggests, even in the acute time ranges, an attempt by the TM tissue to accommodate increased flow (e.g. homeostatic response). Since such a homeostatic response is largely observed in perfusion cultures over many days using the traditional design (Acott et al., 2014a), our data demonstrates that our improved design does not deter this important TM function.

In summary, we report an improved perfusion culture system that utilizes only a corneal rim, and demonstrate the model to be suitable for studying the TM.

Supplementary Material

Refer to Web version on PubMed Central for supplementary material.

Acknowledgement

This study was supported by the National Institute of Health/National Eye Institute Award Number R01EY026962 (WM), R01EY031700 (WM), T35EY031282 (TWC and DKW), and R01EY026048 (VKR), Indiana University School of Medicine Showalter Scholarship (WM), and the Indiana Clinical and Translational Sciences Institute funded, in part by Award Number UL1TR002529 from the National Institutes of Health, National Center for Advancing Translational Sciences, Clinical and Translational Sciences Award (WM), and a Challenge Grant from Research to Prevent Blindness (department of Ophthalmology, Indiana University School of Medicine). The content is solely the responsibility of the authors and does not necessarily represent the official views of the National Institutes of Health.

Abbreviations

AFM	atomic force microscopy
ECM	extracellular matrix
JCT	juxtacanalicular region
IOP	intraocular pressure
POAG	primary open angle glaucoma
TM	trabecular meshwork

References

- Abu-Hassan DW, Li X, Ryan EI, Acott TS, Kelley MJ, 2015. Induced pluripotent stem cells restore function in a human cell loss model of open-angle glaucoma. *Stem Cells* 33, 751–761. [PubMed: 25377070]
- Acott TS, Kelley MJ, Keller KE, Vranka JA, Abu-Hassan DW, Li X, Aga M, Bradley JM, 2014a. Intraocular pressure homeostasis: maintaining balance in a high-pressure environment. *J Ocul Pharmacol Ther* 30, 94–101. [PubMed: 24401029]
- Acott TS, Kelley MJ, Keller KE, Vranka JA, Abu-Hassan DW, Li X, Aga M, Bradley JM, 2014b. Intraocular Pressure Homeostasis: Maintaining Balance in a High-Pressure Environment. *Journal of Ocular Pharmacology and Therapeutics* 30, 94–101. [PubMed: 24401029]
- Acott TS, Kingsley PD, Samples JR, Van Buskirk EM, 1988. Human trabecular meshwork organ culture: morphology and glycosaminoglycan synthesis. *Invest Ophthalmol Vis Sci* 29, 90–100. [PubMed: 3335436]
- AGIS, 2000. The Advanced Glaucoma Intervention Study (AGIS): 7. The relationship between control of intraocular pressure and visual field deterioration. The AGIS Investigators. *Am J Ophthalmol* 130, 429–440. [PubMed: 11024415]
- Cha EDK, Xu J, Gong L, Gong H, 2016. Variations in active outflow along the trabecular outflow pathway. *Experimental Eye Research* 146, 354–360. [PubMed: 26775054]
- Chang YR, Raghunathan VK, Garland SP, Morgan JT, Russell P, Murphy CJ, 2014. Automated AFM force curve analysis for determining elastic modulus of biomaterials and biological samples. *J Mech Behav Biomed Mater* 37, 209–218. [PubMed: 24951927]
- Comes N, Borrás T, 2009. Individual molecular response to elevated intraocular pressure in perfused postmortem human eyes. *Physiol Genomics* 38, 205–225. [PubMed: 19401404]
- Ellingsen BA, Grant WM, 1971. The relationship of pressure and aqueous outflow in enucleated human eyes. *Invest Ophthalmol* 10, 430–437. [PubMed: 5578207]
- Erickson-Lamy K, Rohen JW, Grant WM, 1991. Outflow facility studies in the perfused human ocular anterior segment. *Exp. Eye Res* 52, 723–731. [PubMed: 1855546]
- Erickson-Lamy K, Schroeder AM, Bassett-Chu S, Epstein DL, 1990. Absence of time-dependent facility increase (“washout”) in the perfused enucleated human eye. *Invest. Ophthalmol. Vis. Sci* 31, 2384–2388. [PubMed: 2243003]
- Gerometta R, Podos SM, Candia OA, Wu B, Malgor LA, Mittag T, Danias J, 2004. Steroid-induced ocular hypertension in normal cattle. *Arch Ophthalmol* 122, 1492–1497. [PubMed: 15477461]
- Gerometta R, Podos SM, Danias J, Candia OA, 2009. Steroid-induced ocular hypertension in normal sheep. *Investigative ophthalmology & visual science* 50, 669–673. [PubMed: 18824726]
- Johnson DH, Tschumper RC, 1987. Human trabecular meshwork organ culture. A new method. *Investigative ophthalmology & visual science* 28, 945–953. [PubMed: 3583633]
- Johnson M, Chen A, Epstein DL, Kamm RD, 1991. The pressure and volume dependence of the rate of wash-out in the bovine eye. *Curr. Eye Res* 10, 373–375. [PubMed: 2070641]
- Kasetti RB, Patel PD, Maddineni P, Zode GS, 2020. Ex-vivo cultured human corneoscleral segment model to study the effects of glaucoma factors on trabecular meshwork. *PLoS One* 15, e0232111. [PubMed: 32579557]
- Kazemi A, McLaren JW, Kopczynski CC, Heah TG, Novack GD, Sit AJ, 2018. The Effects of Netarsudil Ophthalmic Solution on Aqueous Humor Dynamics in a Randomized Study in Humans. *J Ocul Pharmacol Ther* 34, 380–386. [PubMed: 29469601]
- Keller KE, Bhattacharya SK, Borrás T, Brunner TM, Chansangpetch S, Clark AF, Dismuke WM, Du Y, Elliott MH, Ethier CR, Faralli JA, Freddo TF, Fuchshofer R, Giovingo M, Gong H, Gonzalez P, Huang A, Johnstone MA, Kaufman PL, Kelley MJ, Knepper PA, Kopczynski CC, Kuchtey JG, Kuchtey RW, Kuehn MH, Lieberman RL, Lin SC, Liton P, Liu Y, Lutjen-Drecoll E, Mao W, Masis-Solano M, McDonnell F, McDowell CM, Overby DR, Pattabiraman PP, Raghunathan VK, Rao PV, Rhee DJ, Chowdhury UR, Russell P, Samples JR, Schwartz D, Stubbs EB, Tamm ER, Tan JC, Toris CB, Torrejon KY, Vranka JA, Wirtz MK, Yorio T, Zhang J, Zode GS, Fautsch MP, Peters DM, Acott TS, Stamer WD, 2018. Consensus recommendations for trabecular meshwork cell isolation, characterization and culture. *Exp. Eye Res* 171, 164–173. [PubMed: 29526795]

- Li H, Bagué T, Kirschner A, Weisenthal RW, Patteson AE, Annabi N, Stamer WD, Ganapathy PS, Herberg S, 2020. A tissue-engineered human trabecular meshwork hydrogel for advanced glaucoma disease modeling. *bioRxiv*, 2020.2007.2031.229229.
- Lindstrom RL, Kaufman HE, Skelnik DL, Laing RA, Lass JH, Musch DC, Trousdale MD, Reinhart WJ, Burris TE, Sugar A, et al. 1992. Optisol corneal storage medium. *Am J Ophthalmol* 114, 345–356. [PubMed: 1524127]
- Loewen RT, Roy P, Park DB, Jensen A, Scott G, Cohen-Karni D, Fautsch MP, Schuman JS, Loewen NA, 2016. A Porcine Anterior Segment Perfusion and Transduction Model With Direct Visualization of the Trabecular Meshwork. *Investigative ophthalmology & visual science* 57, 1338–1344. [PubMed: 27002293]
- Lorenzetti OJ, 1970. Effects of corticosteroids on ocular dynamics in rabbits. *J Pharmacol Exp Ther* 175, 763–772. [PubMed: 5489927]
- Mao W, Tovar-Vidales T, Yorio T, Wordinger RJ, Clark AF, 2011. Perfusion-cultured bovine anterior segments as an ex vivo model for studying glucocorticoid-induced ocular hypertension and glaucoma. *Invest. Ophthalmol. Vis. Sci* 52, 8068–8075. [PubMed: 21911581]
- McDonnell F, Dismuke WM, Overby DR, Stamer WD, 2018. Pharmacological regulation of outflow resistance distal to Schlemm’s canal. *Am J Physiol Cell Physiol* 315, C44–C51. [PubMed: 29631366]
- McKee CT, Last JA, Russell P, Murphy CJ, 2011. Indentation versus tensile measurements of Young’s modulus for soft biological tissues. *Tissue engineering. Part B, Reviews* 17, 155–164. [PubMed: 21303220]
- Morgan JT, Raghunathan VK, Thomasy SM, Murphy CJ, Russell P, 2014. Robust and artifact-free mounting of tissue samples for atomic force microscopy. *BioTechniques* 56, 40–42. [PubMed: 24447138]
- Overby D, Gong H, Qiu G, Freddo TF, Johnson M, 2002. The mechanism of increasing outflow facility during washout in the bovine eye. *Invest. Ophthalmol. Vis. Sci* 43, 3455–3464. [PubMed: 12407156]
- Raghunathan VK, Benoit J, Kasetti R, Zode G, Salemi M, Phinney BS, Keller KE, Staverosky JA, Murphy CJ, Acott T, Vranka J, 2018. Glaucomatous cell derived matrices differentially modulate non-glaucomatous trabecular meshwork cellular behavior. *Acta Biomater.* 71, 444–459. [PubMed: 29524673]
- Rasmussen CA, Kaufman PL, 2005. Primate glaucoma models. *J Glaucoma* 14, 311–314. [PubMed: 15990615]
- Resnikoff S, Pascolini D, Etya’ale D, Kocur I, Pararajasegaram R, Pokharel GP, Mariotti SP, 2004. Global data on visual impairment in the year 2002. *Bull World Health Organ* 82, 844–851. [PubMed: 15640920]
- Shepard AR, Millar JC, Pang IH, Jacobson N, Wang WH, Clark AF, 2010. Adenoviral gene transfer of active human transforming growth factor- β 2 elevates intraocular pressure and reduces outflow facility in rodent eyes. *Investigative ophthalmology & visual science* 51, 2067–2076. [PubMed: 19959644]
- Sherwood JM, Reina-Torres E, Bertrand JA, Rowe B, Overby DR, 2016. Measurement of Outflow Facility Using iPerfusion. *PLoS One* 11, e0150694. [PubMed: 26949939]
- Snider EJ, Boice EN, Gross B, Butler JJ, Zamora DO, 2021. Characterization of an anterior segment organ culture model for open globe injuries. *Sci Rep* 11, 8546. [PubMed: 33879808]
- Stamer WD, Acott TS, 2012. Current understanding of conventional outflow dysfunction in glaucoma. *Curr. Opin. Ophthalmol* 23, 135–143. [PubMed: 22262082]
- Stamer WD, Clark AF, 2017. The many faces of the trabecular meshwork cell. *Exp Eye Res* 158, 112–123. [PubMed: 27443500]
- Torrejon KY, Pu D, Bergkvist M, Danias J, Sharfstein ST, Xie Y, 2013. Recreating a human trabecular meshwork outflow system on microfabricated porous structures. *Biotechnology and Bioengineering* 110, 3205–3218. [PubMed: 23775275]
- Vranka JA, Staverosky JA, Reddy AP, Wilmarth PA, David LL, Acott TS, Russell P, Raghunathan VK, 2018. Biomechanical Rigidity and Quantitative Proteomics Analysis of Segmental Regions of

the Trabecular Meshwork at Physiologic and Elevated Pressures. *Invest. Ophthalmol. Vis. Sci* 59, 246–259. [PubMed: 29340639]

Yemanyi F, Vranka J, Raghunathan V, 2020. Generating cell-derived matrices from human trabecular meshwork cell cultures for mechanistic studies, in: Caballero D, Kundu SC, Reis RL (Eds.), *Methods in Cell Biology*, 1 ed. Academic Press, London, United Kingdom, pp. 271–307.

Zhou EH, Paolucci M, Dryja TP, Manley T, Xiang C, Rice DS, Prasanna G, Chen A, 2017. A Compact Whole-Eye Perfusion System to Evaluate Pharmacologic Responses of Outflow Facility. *Invest. Ophthalmol. Vis. Sci* 58, 2991–3003. [PubMed: 28605810]

Highlights

A glue-based perfusion culture model using corneal rims

Low cost and high availability

An alternative to anterior segment perfusion culture model

Author Manuscript

Author Manuscript

Author Manuscript

Author Manuscript

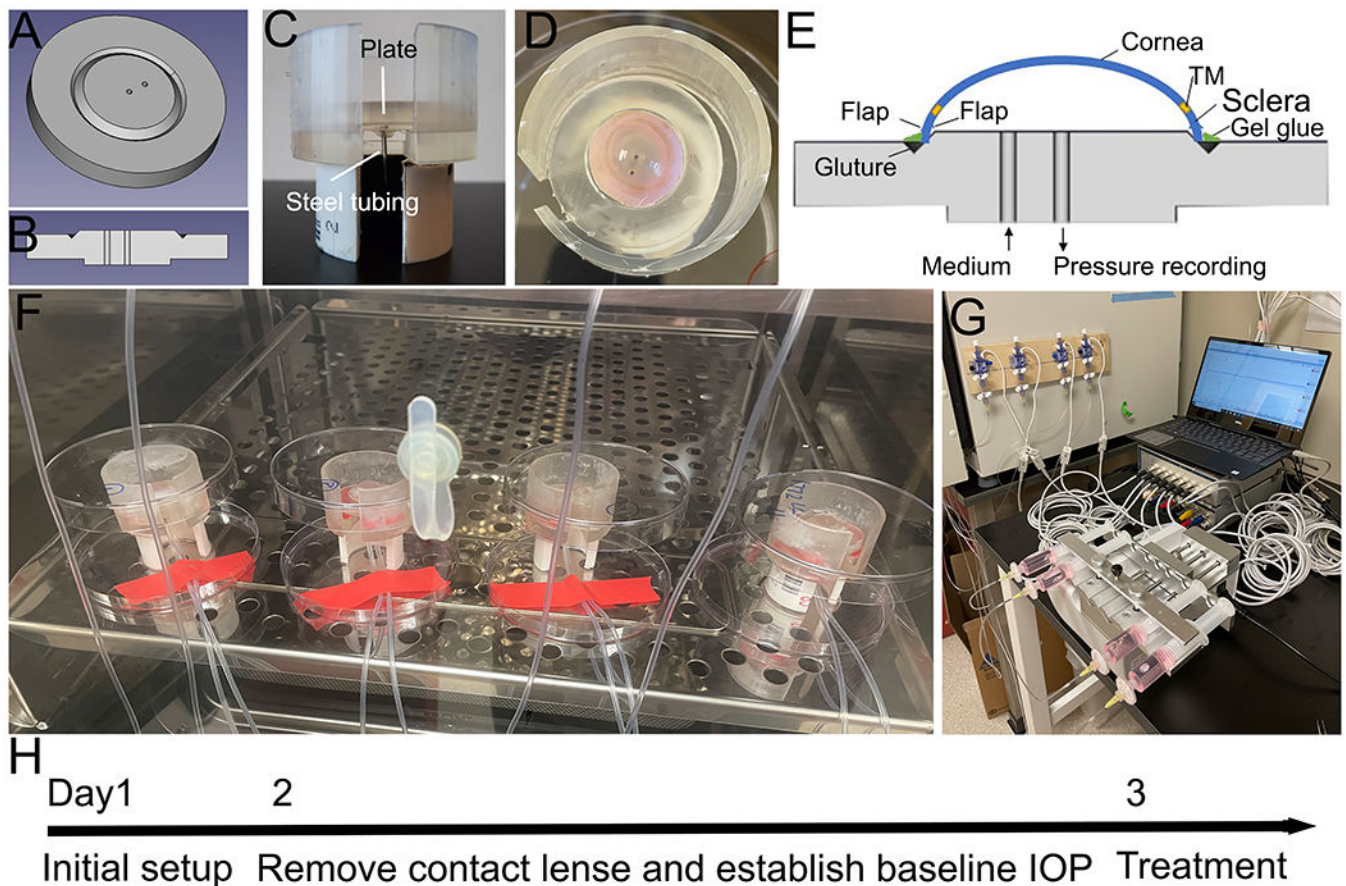


Figure 1.

Corneal rim perfusion culture model setup.

A) Top-down view of the perfusion culture plate. B) Sideview of the plate. C) Sideview of the plate holder and the plate. The plate holder consisted of two parts: the 3D printed top and the PVC bottom (glued together). The plate was placed in the middle. Stainless steel tubing (two pieces) was glued to the plate for plastic tubing connection. D) A corneal rim was mounted onto the plate and placed in a holder. E) A diagram showing how the corneal rim was prepared and glued to the plate. F) A representative image of the mounted corneal rim in the incubator. A petri dish was used as the cover and another one was used to hold medium. G) An automated syringe pump system was connected to the artificial anterior chamber inlet. Pressure transducers were connected to the signal amplifier and bridge amplifier for pressure recordings. H) Timeline of experimental setup.

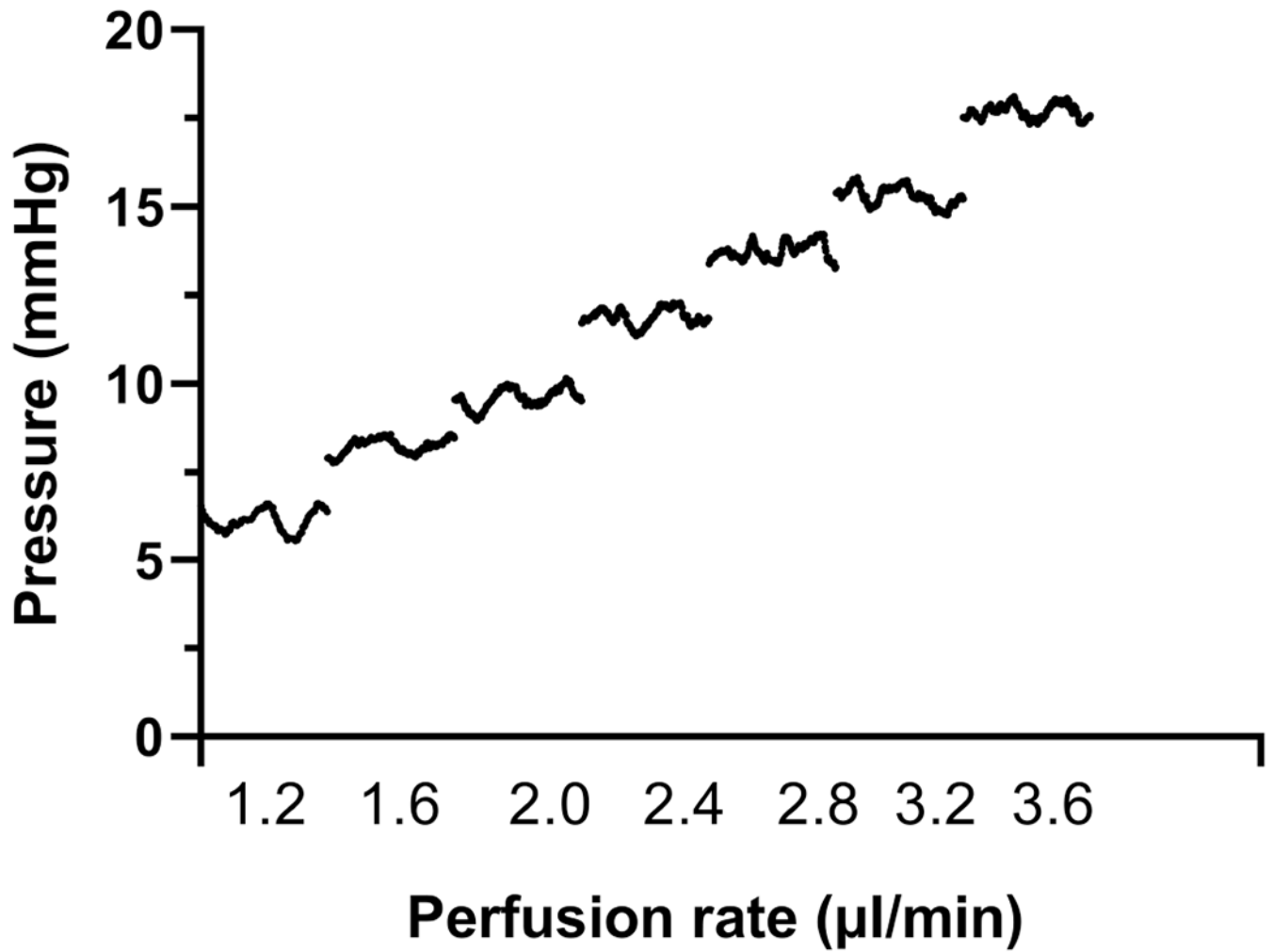


Figure 2. Representative stabilized IOP readings at different flow rates of a represented corneal rim. Perfusion rates were adjusted from 1.2 µl/min to 3.6 µl/min at 0.4 µl/min intervals. IOP data were obtained from a 15-minute rolling average (the last 15 minute) of the 75 minute equilibration time. The stabilization periods were not shown.

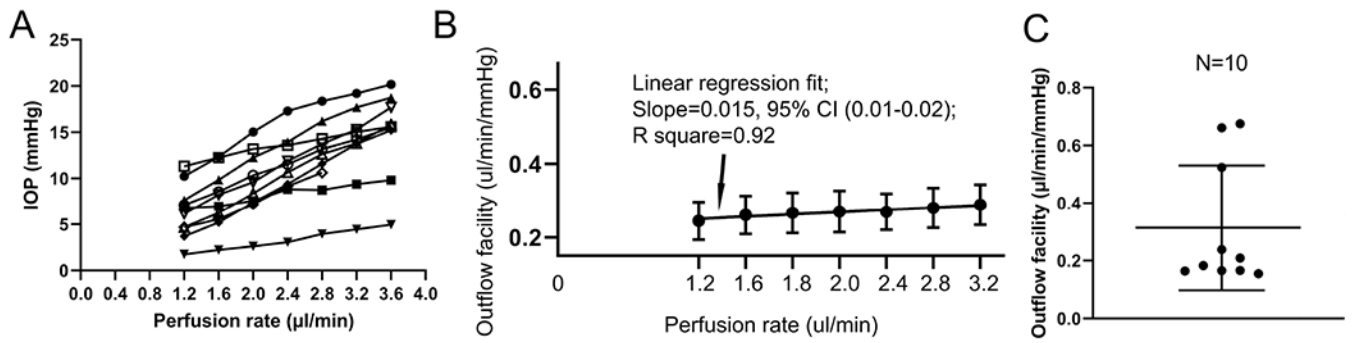


Figure 3.
 Outflow facility measurements.
 (A) Pressure recordings obtained at different perfusion rates of 10 corneal rims. (B) Linear regression fit of mean outflow facility at each perfusion rate. Means and standard errors are shown. N=9 or 10. (C) Outflow facility of the same corneal rims shown in (A). The mean and standard deviations are shown. N=10.

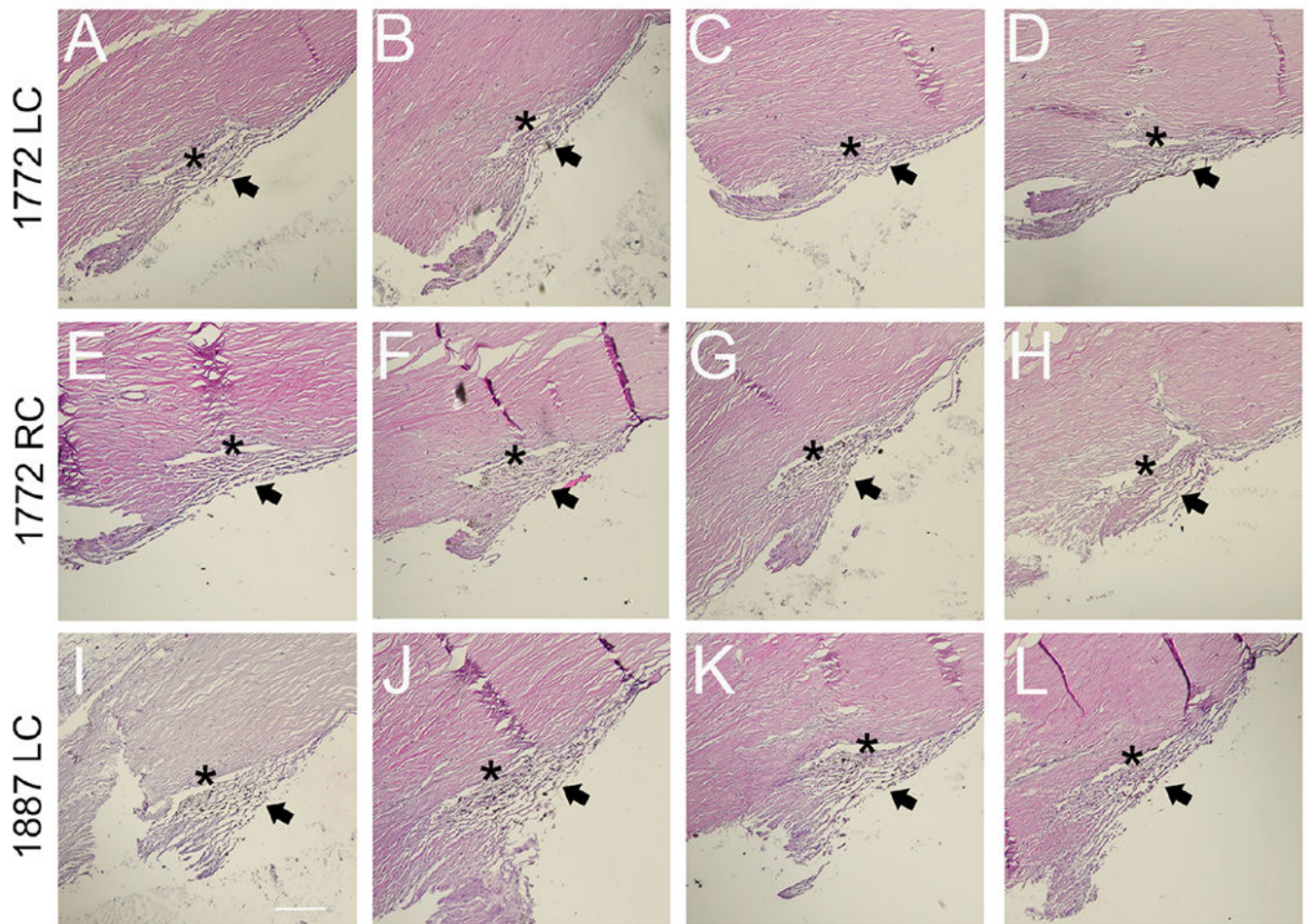


Figure 4. Hematoxylin and eosin staining of the TM region following perfusion culture. Corneal rims were excised from the perfusion plate up to 7 days post perfusion culture and sectioned into four 3mm wide sagittal segments. A representative image is shown for each of the 4 quadrants, and 3 different corneal rims are shown in (A) – (D), (E) – (F), and (I) – (L), respectively. Asterisks: Schlemm’s canal. Arrows: TM.

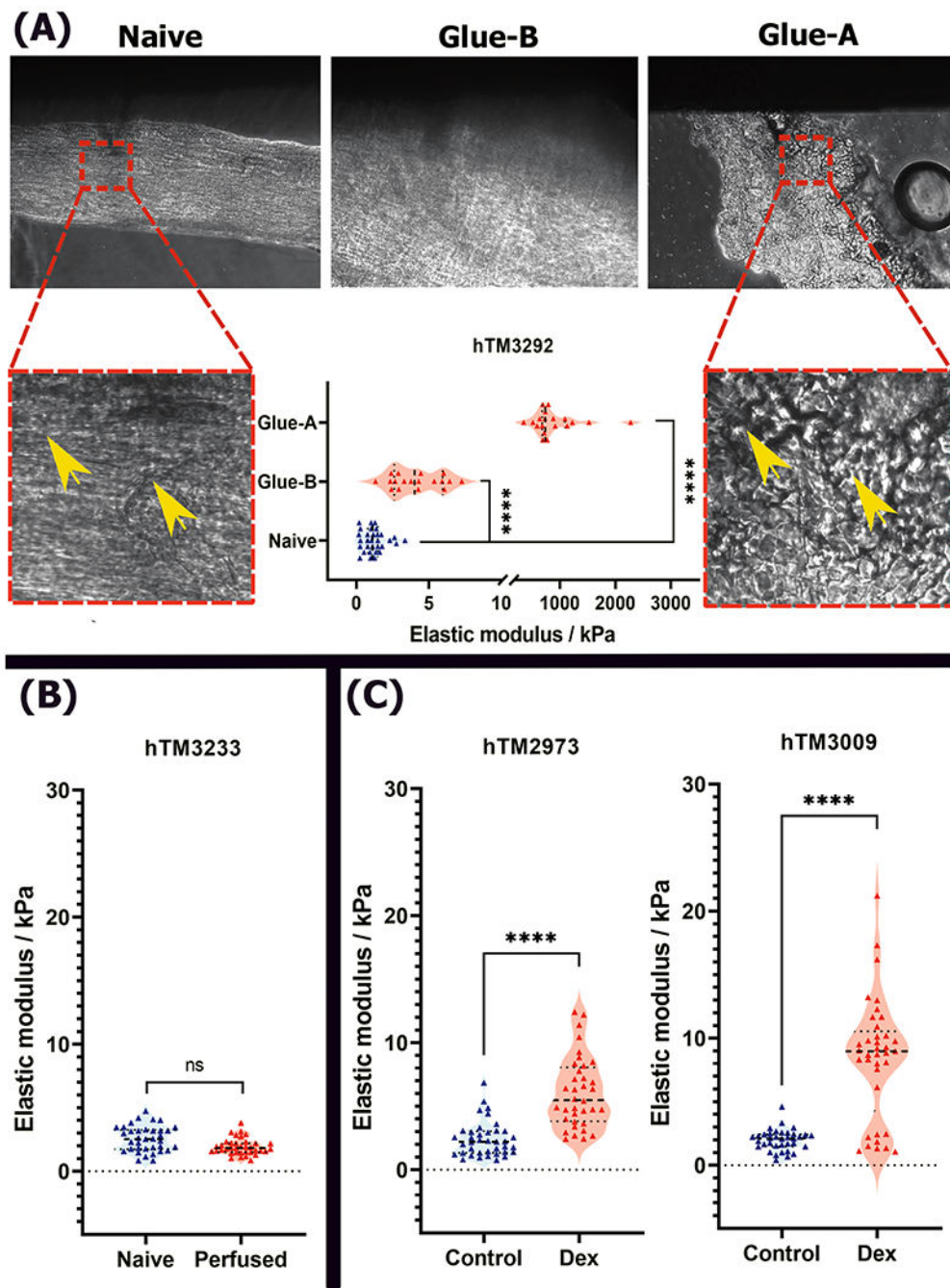


Figure 5. Elastic moduli of TM tissues following perfusion culture with vehicle control or dexamethasone. (A) The effect of permeation of glue on TM elastic modulus. Naïve TM tissue, and multiple regions of TM tissue whose rims were glued into the perfusion chamber were observed under phase contrast in the AFM. Glue A: TM with obvious glue contamination; Glue B: TM with subtle/slight glue contamination. Yellow arrows in the left box region: visible TM beams. Yellow arrows in the right boxed region: glue contamination in the TM. (B) The elastic modulus of the TM of naïve and perfused tissue

without glue contamination. (C) The effect of dexamethasone (Dex) on elastic modulus of TM in perfused tissues. **** $p < 0.0001$, Paired t-test, two-tailed, per donor.

Author Manuscript

Author Manuscript

Author Manuscript

Author Manuscript